Postdoctoral Association
UNIVERSITY OF COLORADO
DENVER | ANSCHUTZ MEDICAL CAMPUS

POSTDOC RESEARCH DAY

July 11th, 2024

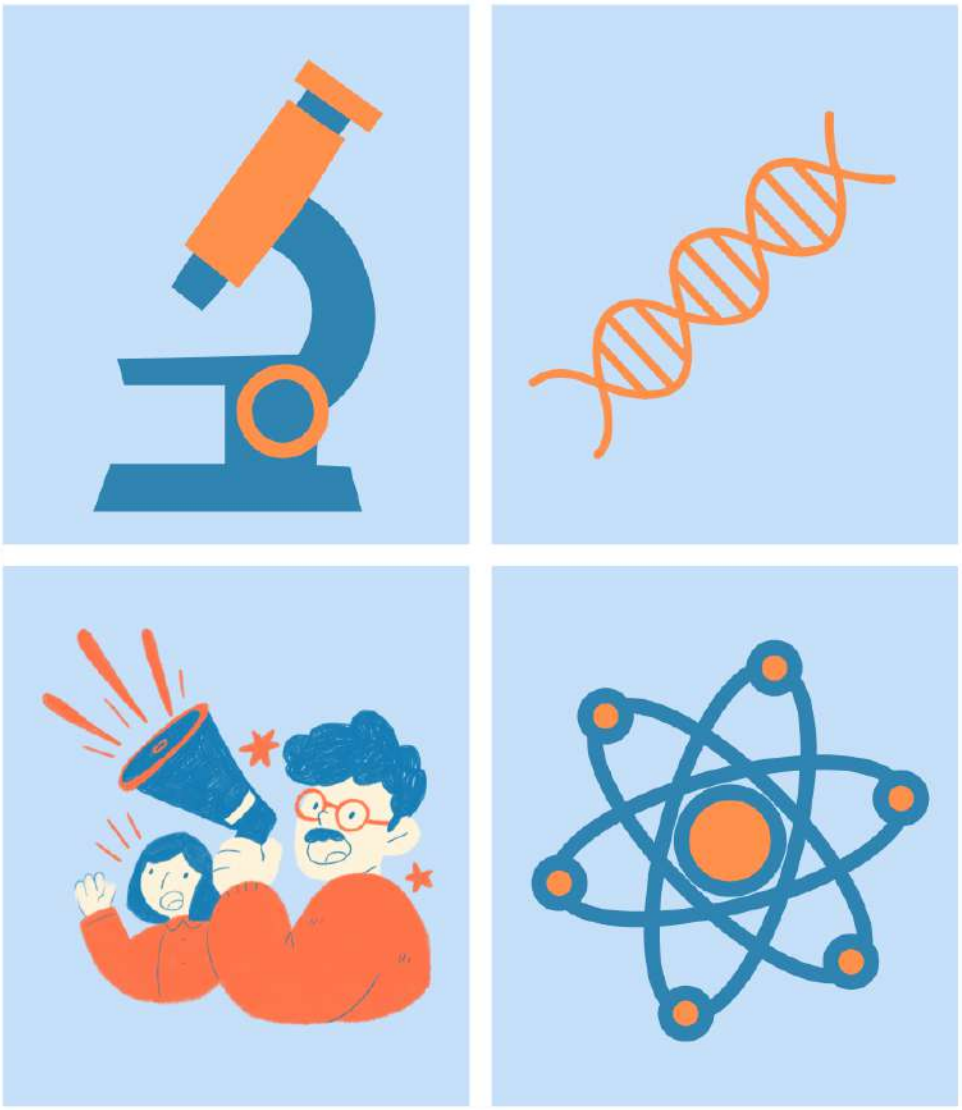

Becoming Agents of Change

Amplifying Postdoc Voices in Research and Beyond

Table of Contents

Program

9:00 am - 10:00 am:	Postdoc Networking Breakfast
10:05 am - 10:10 am:	Opening remarks by **Dr. Roderick Nairn**
10:15 am - 11:15 am:	Keynote presentation – **Dr. Amber Ismael** "Empowered Bites: Making Advocacy Accessible"
11:30 am - 1:30 pm:	Lunch, poster session, and vendor fair
1:35 pm - 1:40 pm:	Remarks by **Dean Richer**
1:45 pm - 3:00 pm:	Keynote Presentation – **Kristan Uhlenbrock** "A Scientist in the Wild: Engaging Outside of Academia and the Lab"
3:15 pm - 4:30 pm:	Anschutz Advocacy Group Expo
4:30 pm - 6:30 pm:	Happy Hour at T-Street

2024 Postdoc Research Day Planning Committee

Lisa Golden, PhD
Chair of Planning Committee

Marycruz Flores Flores, PhD

Yvonne Kumah, PhD

Dominic Shayler, PhD

Sara Stoner, PhD

Erin Golden, PhD
Assistant Director, Postdoctoral Office

Keynote Speakers

Amber Ismael, PhD

Amber Ismael (she/they) is a Senior Program Manager in the Office of Scientific Career Development at the Fred Hutchinson Cancer Center in Seattle, WA. She helps graduate students and postdocs achieve their career goals by providing career and professional development, emphasizing interactive, experiential, and peer learning to provide a more personalized and fulfilling experience. Her experiences as a Ph.D. student and postdoc give her an understanding of early-career scientists' hurdles, and she continues to partner closely with trainees to understand their changing needs. Amber advocates nationally for postdocs and seeks to improve the postdoctoral experience by providing resources and recommendations for postdocs and those who support them through her work with the National Postdoctoral Association. Out in the wild, you will find Amber exploring the Pacific Northwest with her family, mountain biking, trail running, cross-country skiing, or trying to cook the perfect pizza.

Kristan Uhlenbrock, MS

Kristan Uhlenbrock is the Executive Director of the Institute for Science & Policy, a project of the Denver Museum of Nature & Science, where she works to ensure science has a respected role in public discourse and policymaking. She is motivated by life's interesting people, places, problems, and potential for advancing our understanding of the world and the solutions we need to sustain it. For the past two decades, she's worked at the intersection of science, policy, community engagement, and communication for organizations like the University Corporation for Atmospheric Research, the Center for American Progress, the American Geophysical Union, the US Environmental Protection Agency, and the White House. In 2023, she was the recipient of the National Academies Eric & Wendy Schmidt Excellence in Science Communication Award. Kristan values giving back through leadership and volunteer roles, including serving on boards and committees for the AAAS Dialogue on Science, Ethics, and Religion, the American Meteorological Society, the Association of Science & Technology Centers, and the Science Writers Association of the Rocky Mountains Board, as well as being a mentor for the Morgridge Acceleration Program and the Promoting Geoscience Research, Education, and Success Program. She was a CIVIC DNA Fellow and an ASTC Deliberation & Dialogue Fellow. In her free time, Kristan enjoys escaping to the outdoors, writing, and good food and drink with friends.

Advocacy Groups

Project Bridge
The mission of Project Bridge is to foster public interest in primary science research. As scientists, we often find it difficult to express the excitement and importance of our work to our non-science family and friends. This communication barrier is also reflected in the current dour funding climate for primary research projects. As such, we believe that conscious efforts must be made to create new advocates for science research. Project Bridge holds workshops for scientists to strengthen communication skills. We also utilize a grassroots approach to address these issues through our multiple community events. This increased interaction between researchers and their community will increase the appreciation and understanding of the importance of scientific research.
https://www.cuanschutz.edu/services/project-bridge

Josepha's Kapamilya for Outreach and Advancement (J-KOA) in STEAM
We are Josepha's Kapamilya for Outreach & Advancement in STEAM, or J-KOA for short.

Our mission is to serve our communities in whatever way we can. We do this by empowering the next generation of scientists and engaging in science outreach. Beyond that, we also work as an outreach branch of the Denver Metro Regional Science and Engineering Fair (DMRSEF) promoting the fair to grade school students.

Society for the Advancement of Chicanos/Hispanics and Native Americans in Science (SACNAS)
SACNAS is an organization that encourages the inclusion and diversity in STEM and in the community. Our goals are expanding our networks, chapters and memberships; impacting STEM career development and representation at all levels through expanded awareness, access and resources; and having an influence diversifying the STEM enterprise.
https://www.cuanschutz.edu/services/sacnas

Women in STEM (WiSTEM)
CU Anschutz Women in STEM (WiSTEM) is a student and staff-run organization whose goal is to substantially increase the representation of women in STEM disciplines through advocacy, education, community outreach, skill building, and fostering allies among our peers.

We are committed to cultivating discussions on issues in STEM fields, promoting mentorship opportunities, providing career development resources, and being involved in our community. Our events host participants at the K-12, undergraduate, and medical campus-level.
https://www.cuanschutz.edu/services/women-in-stem/home

Postdoctoral Association (PDA)
The goals of the PDA are to address the needs and concerns of postdoctoral fellows within the institution by promoting postdoctoral advocacy, career development, and community development.
https://www.cuanschutz.edu/services/postdoc-association

Abstracts

1. **Peptidoglycan deficiency and cell wall permeability of phage-resistant Enterococcus faecium leads to antibiotic sensitization.** Arya G., Espinosa J., Chodisetti P, Hang H., Duerkop B.

   Enterococcus faecium is a commensal of the human intestine and an opportunistic pathogen that causes multidrug resistant (MDR) nosocomial infections. Bacteriophages (phages) have been proposed as potential therapeutics for the treatment of multidrug resistant infections. A major obstacle for phage therapy is the emergence of phage resistant bacteria. However, phage resistance can impact bacterial fitness resulting in antibiotic sensitization, reduced virulence, and host colonization defects. Understanding fitness costs that come with phage resistance will help inform phage therapies and can likely be leveraged as an antimicrobial strategy. We discovered that phage resistant E. faecium harbor mutations in the cell wall hydrolase gene sagA. SagA cleaves crosslinked peptidoglycan (PG) and is involved in PG remodeling. We show that phage mediated mutations in sagA compromises E. faecium PG hydrolysis rendering them sensitive to the cephalosporin ceftriaxone. Using SDS lysis and chlorophenol-red β-d-galactopyranoside (CPRG) hydrolysis assays we show that sagA mutants have compromised cell wall integrity and increased cellular permeability. Additionally, E. faecium sagA mutants are more reactive to Bocillin-FL (fluorescently-labeled penicillin), a β-lactam like ceftriaxone which acylates penicillin binding proteins (PBPs), suggesting that cell wall permeability leads to elevated PBP inactivation and heightened sensitivity to β-lactams. Finally, E. faecium sagA mutants showed non-uniform distribution of newly synthesized PG in their cell wall and amorphous cell shape compared with wild type cells. These findings further implicate cell wall synthesis deficiencies in ceftriaxone sensitivity and show that by altering a single PG hydrolase, E. faecium loses intrinsic cephalosporin resistance. Understanding the mechanistic basis of loss of SagA function and cephalosporin sensitization will inform how phages could serve in combination therapy to restore cephalosporin activity against MDR E. faecium.

2. **The Role of SCZ GWAS Gene Akt3 in Recency Discrimination Memory, Locomotive Behavior and Brain Size in Females.** Barbee, BR; Howell, K; Bellemare, K; Law, AJ.

   Genome-wide association studies have implicated the AKT3 gene as a key contributor to schizophrenia (SCZ) risk as well as treatment efficacy with antipsychotic drugs. Our prior work (Howell et al., 2017, PLoS One) found that male Akt3 genetically-deficient mice were hyperlocomotive and exhibited deficits in recency discrimination memory. However, these behaviors have not been examined in female mice, relevant because female subjects have largely been neglected in preclinical studies of SCZ. We used female (3–5-month-old) Akt3 wild-type (Akt3+/+), Akt3 heterozygous (Akt3+/-) and Akt3 knockout (Akt3-/-) mice. Brain size and brain/body weight ratio were assessed in behaviorally-naïve mice. The open field test assessed locomotor activity and anxiety-like behavior. The temporal order object recognition memory task assessed recency discrimination memory. Female Akt3-/- mice have reduced brain weight and a lower brain/body weight ratio. We identified a trending main effect of genotype in total overall distance traveled,

indicating that Akt3-/- female mice were hyperlocomotive. There were no differences in time in center or center distance traveled, suggesting no anxiety-like phenotype. Female mice did not exhibit obvious recency discrimination memory deficits. We confirm that female Akt3-/- mice have reduced brain size and a lower brain/body weight ratio (but no difference in body weight), consistent with that observed in males and supportive of a role for Akt3 in the attainment of typical brain size. In addition, female Akt3-/-mice are hyperlocomotive, replicating our prior male data. Conversely, unlike males, female genetically-deficient Akt3 mice exhibit intact recency discrimination memory. Future studies are oriented to more thorough characterization of sex differences within this genetic rodent model, including social behavior and fear learning and memory. This work was supported by 5R01MH103716 (AJL), T32-MH015442-44 (BRB, AJL), and Developmental Psychobiology Endowment Fellowships to BRB and KH.

3. **Long non-coding RNA in IPF: Regulatory players in pulmonary disease.** A. C. Button[1], R. Z. Blumhagen[1], I. V. Yang1, D. A. Schwartz[1]

[1]Department of Medicine, University of Colorado, Aurora, CO, United States

Rationale: Idiopathic pulmonary fibrosis (IPF) is a chronic progressive fatal fibrosing interstitial pneumonia, characterized by relentless progression of respiratory insufficiency. The median survival of IPF has remained between 2-5 years even with the introduction of anti-fibrotics. Despite the progress from extensive work on the protein-coding genes in IPF, there is no clear explanation for the molecular heterogeneity of IPF or the low penetrance of either the MUC5B promoter variant or the other common IPF risk variants in this rare disease. We are working to bridge this gap by investigating the non-coding transcriptome of IPF and the regulatory pathways of the disease. Methods: Published bulk (GSE173355) and single cell (GSE136831 and GSE135893) RNA-seq datasets were re-analyzed and used to identify dysregulated long non-coding RNA (lncRNA) between IPF lungs and control lungs in both bulk lung tissue and in individual cell-types. A subset of these genes was identified for follow-up based on differential expression in IPF epithelial cells. This subset is being subjected to a pooled CRISPRa screen in A549 to identify phenotypes of ER stress, cell death, and autophagy by flow cytometry. These pathways were chosen for their relevance in the IPF lung. Results from the CRISPR screen are being validated by immunoblots for p62/Vimentin/α-SMA, MTT assay, and RNA-seq in both A549 and primary airway epithelial cells. Results: Over 1000 lncRNAs were found to be significantly dysregulated in IPF (adjusted p-value <0.05, fold-change > 2). Of this set, approximately 130 were also dysregulated at the single cell level across multiple scRNA-seq datasets and were used for the CRISPRa screen. Example violin plots from this dataset of lncRNAs LINC00511, PVT1, and AQP4-AS1 are shown in Figure 1. Our CRISPRa screen is ongoing and has already identified several lncRNAs that promote cell death, autophagy, and ER stress as measured by live/dead staining, lysotracker, and ProteoSTAT. These results were validated by GapmeR knockdown and additional phenotypic assays. RNA-seq showed that the differential expression of these lncRNA alters the transcriptome, indicating that each has a unique mechanism by which it influences IPF. Conclusion: We have identified specific lncRNAs that are dysregulated in the IPF lung and whose dysregulation alters the IPF transcriptome and molecular phenotypes. LncRNAs are key players in the general

dysregulated transcriptome present in IPF. Their ability to modulate the transcriptome presents a target in controlling the molecular phenotypes of IPF.

4. **Unraveling the Origins of Recruited Group 2 Innate Lymphoid Cells**. Can, UI; Reinhardt, RL.

   Group 2 innate lymphoid cells (ILC2s) are pivotal in type 2 immune response, crucial for allergies, defense against helminths, and tissue repair. Mainly residing in barrier tissues like the lung, intestine, and skin, ILC2s act as sentinels, detecting and responding to environmental signals. Lung ILC2s consists of tissue-resident natural ILC2s (nILC2s), and migratory inflammatory ILC2s (iILC2s) recruited during mucosal damage or infections. In helminth-induced lung injury, iILC2s emerge by day 5, becoming the early source of type 2 cytokines. However, their origin remains unclear. To explore lung, small intestine (SI), and bone marrow (BM) contributions to origins of iILC2s, we conducted a time-course analysis. Results indicate the lung and BM are unlikely major sources, while the SI remains a strong candidate. Additionally, photoconversion surgeries, of the SI or BM, using Kikume Green-Red mice to locally label and track cells showed that SI cells manifest in the lung as iILC2s, whereas BM cells appear to contribute to nILC2s. In support, adoptively transferred BM progenitors became nILC2s, as expected, but did not give rise to iILC2s. Lastly, scRNA sequencing for lung and mesenteric lymph node ILC2s and BM ILC2 progenitors corroborated our findings. In summary, (1) lung does not appear to be a prominent source for either nILC2s or iILC2s, (2) BM may serve as an origin for nILC2s, but it does not serve as a major source for iILC2s, and, (3) SI is the primary origin of iILC2s.

5. **Early life lipid overload in Native American Myopathy is phenocopied by stac3 knockout in zebrafish.** Rajashekar Donaka; Postdoc, Houfeng Zheng, Cheryl L Ackert-Bicknell, PI, and David Karasik, PI.

   Understanding the early stages of human congenital myopathies is critical for proposing strategies for improving skeletal muscle performance by restoring the functional integrity of cytoskeleton. SH3 and cysteine-rich domain 3 (STAC3) is a protein involved in nutrient regulation, and is an essential component of the excitation-contraction (EC) coupling machinery for Ca2+ releasing. A mutation in STAC3 causes debilitating Native American Myopathy (NAM) in humans, and loss of this gene in mice and zebrafish (ZF) results in death in early life. Clinically, NAM patients demonstrated increased lipids in skeletal muscle, however, whether elevated neutral lipids alter muscle function in NAM disease is not clear. Using a CRISPR/Cas9 induced stac3-/-/knockout (KO) ZF model, we determined that loss of stac3 leads to delayed larval hatching which corresponds with muscle weakness, decreased whole-body Ca2+ level at 3, 4, and 5 days post-fertilization (dpf). Specifically, we observed defects in the cytoskeleton in F-actin and slow muscle fibers at 5 and 7 dpf. Myogenesis regulators such as myoD and myf5, mstnb were significantly altered in stac3-/- larvae, and neutral lipid levels were elevated starting at 5 dpf and persisting beyond 7 dpf. Larva lacking stac3 had reduced viability, and no larva knockouts survived past 11 dpf. These data suggest that stac3-/- zebrafish may serve as an appropriate model to study the diminished muscle function seen in NAM patients.

Keywords: Native American Myopathy, muscle weakness, neutral lipids, zebrafish.

6. **Polymer Coatings to Combat Microbial Growth on 3D Printed Denture-Base Materials.** Escobedo, H.; Salazar, A.; Stansbury, J. W.; Schurr, M.; Nair, D.P.

Purpose

While denture can restore function and confidence in individuals, they often lead to oral complications such as tooth decay, gum disease, yeast infections and pneumonia (Du, Ren et al. 2022). The aim of this in vitro study is to investigate the potential benefits of incorporating acrylated hydroxy azobenzene (AHA) in 3D printed denture-based resins to inhibit oral infections such as denture stomatitis.

Methods & Materials

The inkjet 3D printing formulation consisted of mono-urethane di(meth)acrylate (MUDMA), benzyl urethane methacrylate (BzUMA), dimer acid diisocyanate ethoxy dimethacrylate (DDI-HEMA), and methacrylic acid (MAA) at 34-, 25-, 19-, and 22-wt% respectively (henceforth referred to as inkjet). Two-parts of this formulation were used to create a redox initiating system with benzoyl peroxide (2wt% or 4wt%) and ethyl-4-(dimethyl amino) benzoate (1wt% or 2wt%) in the presence or absence (control) of 2wt% AHA within 0.8mm x 6.5mm (thickness x diameter, V = 26.55 mm3) spacer. The polymerization was initiated at room temperature and completed within the Curebox Plus™ (1h at 80°C under ultraviolet light 365nm & 405 nm, 36 Watts). For the Candida albicans (C. albicans) assay, sterile samples were incubated statically with 1.8×105 colony-forming-units (CFU/mL) for 13h at 37°C and 5% CO2 followed by detaching the biofilm growth on the samples in a water suspension via mechanical force (vortex and sonication) and quantifying CFU. For the Streptococcus mutans (S. mutans) study, sterile samples were incubated on agar plates spread with 4×105 CFU/mL and grown for 24h at 37°C and 5% CO2. The zone of inhibition radii was measured. Cytocompatibility of the samples were studied via MTT assay using direct contact with human gingival fibroblasts (HGF) cells. Number of samples $n \geq 3$.

Results

The AHA-inkjet samples showed a 12-fold reduction in C. albicans biofilm growth compared to the control inkjet samples ($p < 0.05$). For the S. mutans study, the AHA-inkjet sample inhibited bacterial growth and demonstrated a zone of inhibition (10.2 mm ± 0.30 mm), which were absent in the control samples. Both AHA- and control-inkjet samples were not significantly different ($p > 0.05$) in metabolic activity compared to only HGF cells.

Conclusion

AHA-based 3D printed denture-base materials can significantly inhibit the growth of C. albicans and S. mutans, thereby giving the potential to remediate risks and complications from removable dental prosthesis. The next phase of the study will focus on quantifying the transient, light-induced mechanical movement of AHA samples (photofluidization effect) from the surface of the dentures to enable biofilm disruption from the surface of the material.

7. **Histone deacetylase 8 modulates myofibril relaxation.** Jones, TLM; Hoffer, C; Wilson, CE; Fritz, K; Delligatti, CE; Kirk, JA; Walker, LA; McKinsey, TA; Woulfe, KC.

   Background: Heart failure with preserved ejection fraction (HFpEF) currently accounts for over 50% of all heart failure diagnoses and the prevalence is growing. HFpEF is characterized by insufficient cardiac output due to diastolic dysfunction. Multiple factors contribute to impairment of cardiac relaxation in HFpEF, including increased fibrosis, abnormal calcium handling, and sarcomere dysfunction. Previous studies have demonstrated that increasing sarcomeric acetylation by globally inhibiting histone deacetylase (HDAC) isoforms accelerates myofilament relaxation, thereby improving overall diastolic function; however, the particular HDAC isoform that regulates sarcomeric relaxation is unknown.
   Hypothesis: We hypothesize that sarcomeric relaxation is modulated by specific HDAC isoforms and that identification of the specific isoforms will allow for precise therapeutics for the improvement of cardiac relaxation.
   Methods: Adult rat ventricular myocytes (ARVMs) were isolated and treated with inhibitors that specifically inhibit HDAC isoforms. Cellular dynamics, myofilament acetylation, and myofibril function were measured.
   Results: ARVMs treated with 10nM PCI-34051, an HDAC8 inhibitor, for 24 hours had increased myofilament acetylation and faster cellular relaxation (normalized tau: DMSO 1.03 ± 0.04; PCI-34051 0.79 ± 0.03; p = 0.001). In contrast, the cellular relaxation of ARVMs treated with 1μM MGCD-0103, 1μM TMP-195, or 1 μM Tubastatin A (inhibitors of other HDAC isoforms) was not significantly different. Myofibrils isolated from ARVMs treated with PCI-34051 had faster relaxation kinetics than myofibrils from ARVMs treated with DMSO (normalized linear relaxation: DMSO 1.0 ± 0.08; PCI-34051 0.58 ± 0.09; p = 0.006); whereas myofibrils isolated from ARVMs treated with other HDAC inhibitors did not. Moreover, myofibrils treated with recombinant HDAC8 had decreased myofilament acetylation and prolonged relaxation kinetics (normalized linear relaxation: DMSO 1.0 ± 0.13; rHDAC8 1.97 ± 0.05; p = 0.048).
   Conclusions: This study demonstrates that HDAC8 specifically modulates myofibril relaxation through the deacetylation of sarcomeric proteins. Inhibiting HDAC8 to accelerate myofibril relaxation has the potential to improve diastolic function in HFpEF patients through a novel regulatory pathway.

8. **Activation of Ca2+-permeable AMPARs are required for structural plasticity induced by sTBS in the mouse hippocampus.** Laura Koek, Gregory Bond,Thomas Sanderson, John Georgiou, Benjamin Scholl, Graham Collingridge.

   Long-term potentiation (LTP) at hippocampal CA3-CA1 synapses, can be subdivided into two mechanistically different forms of NMDAR-dependent synaptic potentiation based on their independence of (LTP1) or dependence on (LTP2) de novo protein synthesis (PS). Previous experiments reported the requirement of CP-AMPAR activation and intracellular calcium stores for LTP2 but not LTP1. Here the requirement for CP-AMPARs and intracellular calcium stores in structural LTP (sLTP) were investigated. Simultaneous field potential recordings and two-photon imaging were carried out in

acute hippocampal slices of adult mice (P70-100) expressing Thy1-EGFP. Additionally, FM 4-64 was used to label presynaptic boutons of activated synapses3. Two TBS protocols (3xTBS) with different inter-episode intervals (IEI) were used – a compressed TBS (cTBS) protocol (IEI 10 s) to induce LTP1 and a spaced TBS (sTBS) protocol (IEI 10 min) to induce LTP2 and LTP1. Custom written scripts in MATLAB and python were used to automate the analysis of sLTP. Throughout the 3h recording session, both spine fluorescence and synaptic transmission remained stable. This persistent increase in spine volume induced by sTBS, was prevented by treatment with D-AP5 (50 μM), anisomycin (30 μM), ryanodine (10 μM), IEM- 1460 (30 μM), suggesting that activation of NMDARs, de novo PS, CP-AMPARs and intracellular calcium signalling are vital for sLTP.

9. **Modulating Enzyme Function via Dynamic, Allostery and structure changes within Biliverdin Reductase B.** Lee, E; Redzic, J; Eisenmesser, E.

   Biliverdin reductase B (BLVRB) is an NADPH-dependent oxidoreductase that catalyzes the reduction of multiple substrates. BLVRB plays a crucial role in redox regulation, with the enzyme alone determining the fate of hematopoietic cells. The high expression of BLVRB in cancer cells suggests its involvement in cancer cell proliferation. However, the precise role of BLVRB's structure, dynamics, and allostery throughout the catalytic cycle has remained elusive. In this study, we have uncovered key insights into Apo BLVRB structure, particularly focusing on residue R78, which plays a crucial role in interacting with the coenzyme. Our findings reveal that in the absence of the coenzyme, R78 exhibits high flexibility from both X-ray crystallography and NMR. However, upon coenzyme binding, R78 adopts a stable closed conformation through the formation of a hydrogen bond with T12 CO. This conformational change leads to a reduction in protein dynamics, including the R78 loop, across both fast and slow timescales. Furthermore, we have identified that the stereochemistry of the coenzyme is altered by oxidation states, leading to significant conformational changes throughout the entire enzyme. These findings offer valuable insights into both the structural and dynamic aspects of BLVRB and contribute to our understanding of its functional role in redox regulation. Moreover, our study reveals an intriguing discovery regarding residue 164. Despite its distance from the active site (>26 Å), we have observed that a single-site evolutionary mutation at position 164 induces remarkable structural rearrangements. This unexpected finding highlights the pivotal role of residue 164 in controlling the function and dynamics of BLVRB. It suggests that the fine-tuned allosteric site at position 164 plays a crucial role in regulating the activity of the enzyme. In summary, our study not only provides insights into the structural and dynamic characteristics of BLVRB but also highlights the importance of residue 164 as a key determinant of its function and allosteric regulation. These findings contribute to a deeper understanding of BLVRB's mechanisms and open avenues for further research in the field.

10. **Hypoxic Pregnancy Alters the Metabolome and Transcriptome and Promotes Fibrosis in the Ovine Fetal Liver.** McGuckin, MM(1); Ortiz, JL(1); Wang, D(1); Dobrinskikh, E(1); Tong, W(2); Botting, KJ(2); Niu, Y(2); Giussani, DA(2); and Wesolowski, SR(1)
(1) University of Colorado Anschutz Medical Campus, Aurora, CO, USA
(2) University of Cambridge, Cambridge, UK

Introduction: Fetal hypoxemia is a common pregnancy complication associated with fetal growth restriction (FGR). In turn, FGR offspring have a higher risk for liver metabolic disease. Our objective was to gain a better understanding of how hypoxemia disrupts metabolism and development in the fetal liver. We hypothesized that hypoxemia activates nutrient and oxidative stress pathways and shifts substrate metabolism in the fetal liver.

Methods: Pregnant ewes were housed in isobaric chambers under normoxia (CON, N=9) or hypoxia (10% O2; HOX, N=7) conditions for 33 d (gestation d 105-138; term is 145 d). Liver biopsies were either fixed in 4% paraformaldehyde for histology or flash frozen for molecular analyses. We performed liver metabolomics and transcriptomics to determine regulated pathways, performed assays to validate stress and nutrient signaling activation, and used picrosirius red staining to identify collagen. Data were analyzed by MetaboAnalyst, R package DESeq2, or Student's t-test.

Results: HOX fetuses had 1.3-fold higher hemoglobin concentration (Hgb, $P<0.01$) and 25% lower bodyweight versus CON ($P<0.01$). In liver tissue, we identified 41 regulated metabolites ($Q<0.10$) including ascorbate, acyl-carnitines, and urate, and 11 enriched pathways ($P<0.10$) including purine, tryptophan, and sphingolipid metabolism. There were 487 regulated genes ($Q<0.15$) and 22 enriched pathways ($P<0.10$) including granzyme A signaling, vitamin C recycling, mitochondrial dysfunction, and oxidative phosphorylation. HOX livers had higher protein expression of gluconeogenic enzymes PCK1 (1.5-fold, $P=0.03$) and G6PC (1.3-fold, $P=0.08$), higher lactate dehydrogenase expression (2.2-fold, $P=0.02$) and activity (1.1-fold, $P=0.06$) and pyruvate dehydrogenase activity (1.8-fold, $P<0.01$). Phosphorylation of mTORS2448 (1.4-fold, $P=0.04$) and its downstream regulator ph-4E-BP1Thr37/46 (1.5-fold, $P=0.04$) were greater in HOX fetal liver. There was higher ph-AMPKT172 (1.4-fold, $P=0.03$) in HOX fetal liver, but no difference in ph-JNKT183/Y185, oxidative phosphorylation complexes, or in the mitochondrial antioxidant SOD2. Histologically, HOX fetuses had greater liver collagen deposition in periportal regions (1.4-fold, $P=0.03$), correlated with Hgb ($P<0.01$, $R2=0.62$) and hepatic levels of the stress metabolite urate ($P<0.01$, $R2=0.66$).

Conclusion: Fetal hypoxemia for 33 d in late gestation upregulated pathways mediating stress signaling and mitochondrial function, and increased periportal collagen deposition. These data provide new insight into how pregnancy complicated by fetal hypoxemia may trigger a postnatal increased risk of hepatic metabolic disease.

Supported by the British Heart Foundation and the National Institutes of Health

11. **Risk and protective alleles differ in their binding potential towards the target autoantigens important in the development of Multiple Sclerosis.** Manjula Miglani[1,3], Vibha Jha[1,3], Elizabeth R. Sunderhaus[1,3], Brian M. Freed[1,2,3], and Christina L. Roark[1,3],*

[1]Department of Medicine, [2]Department of Microbiology and Immunology, [3]ClinImmune Cell and Gene Therapy, University of Colorado, Anschutz Medical Campus, Aurora CO 80045.

Multiple Sclerosis (MS) is an autoimmune disease of the central nervous system where T cell responses against proteins found in the brain result in neurodegenerative disease. The disease has a strong genetic association attributed to HLA Class II alleles, DRB1 and DQB1. HLA-DRB1*15:01 is strongly associated with susceptibility to MS yet the mechanism by which it induces MS is not fully understood. In addition, alleles associated with protection against MS have not been well studied. To identify the most significant alleles associated with MS, a Chi-square analysis was performed comparing the frequency of DRB1 and DQB1 alleles in 1658 MS patients versus 99962 ethnically matched controls (ImmPort SDY1045). DRB1*15:01 was most strongly associated with susceptibility (OR= 1.81, p <0.0001) and DRB1*07:01 (OR= 0.80, p=0.0003) and DRB1*14:01 (OR= 0.61, p=0.0001) were significantly associated with resistance. For DQB1, DQB1*06:02 was most strongly associated with risk and DQB1*02:01, DQB1*05:03, and DQB1*03:03 were associated with protection. Each DRB1 and DQB1 allele was cloned and individually expressed in the HLA class II-deficient T2 cell line to compare binding of two peptides associated with MS, MBP83-101 and RASGRP278-87. Myelin basic protein (MBP) is an important component of myelin sheath that gets degraded in MS. RAS guanyl releasing protein 2 (RASGRP2) is a target autoantigen that is expressed in the cortical grey matter and striatal neurons in the brain. Binding of MBP83-101 and RASGRP278-87 were measured on cell lines individually expressing DRB1*15:01, DRB1*14:01, and DRB1*07:01. DRB1*15:01 bound MBP83-101 strongly (MFI=33450) while the resistant DRB1 alleles bound much less peptide (MFI=2693). For RASGRP278-87, the susceptible DRB1*15:01 allele bound the most peptide (MFI=7619) while the alleles associated with protection bound weakly (MFI=608). Protection from MS correlates with DRB1 alleles that do not strongly bind MBP83-101 and RASGRP278-87. We found that the statistical data obtained from chi-square analysis correlates with the peptide binding data.

12. **Inhibition of Ionic Currents by Fluoxetine in Vestibular Calyces in Different Epithelial Loci.** Maria Pogue, D.O.; Veronica M. Butler, B.S.; Gregory Ottenberg, Reed Ayers, PhD; Christopher Kleck, M.D.; David Ou-Yang, M.D.; Gowrishankar Muthukrishnan, PhD; Cheryl Ackert-Bicknell, PhD.

1. Department of Orthopedics, School of Medicine, University of Colorado, Aurora Colorado
2. Colorado Program for Musculoskeletal Research, University of Colorado, Aurora, Colorado
3. Center for Musculoskeletal Research, University of Rochester, Rochester, NY

Post-operative spinal infections are associated with high rates of morbidity and mortality. Post-operative infections are monitored by fever, pain, neurological changes, and serum

inflammatory markers (CRP and ESR). The long-term goal of this study is to develop between diagnostic markers to monitor post-operative infections. We collected whole blood samples from patient undergoing known spinal hardware revision surgery. PMBCs were isolated, washed, and cells were removed and counted. WBC fractions were analyzed at baseline, two weeks, six weeks, three months, and six months. WBC fractions were not different at baseline between infected and non-infected patients. Using linear discriminate analysis, PBMS numbers had a better infection type than classical clinical variables.

13. **Genetic Suppression of E-cadherin Represses EMT in an Early Lobular-like Tumorigenesis Model.** Musick, MM; Ufondu, CU; Ostrander, JO; Sikora, MJ.

    Invasive lobular carcinoma (ILC) is the most common special histological subtype of breast cancer (~15%; ~40,000 US women/yr), but is understudied relative to breast cancer of no special type (i.e. invasive ductal carcinoma, IDC). The unique molecular mechanisms involved in ILC tumorigenesis -i.e. the progression from atypical lobular hyperplasia (ALH) to lobular carcinoma in situ (LCIS) to ILC- are not well understood, which confounds patient risk evaluation and treatment. E-cadherin loss, a hallmark of ILC, is an early and nearly universal event in ILC and associated precursor lesions (e.g. ALH and LCIS). Studies to date strongly support that E-cadherin has direct tumor suppressor roles that are pivotal to breast tumorigenesis, but mechanistic studies in human cells are limited. To model early ILC tumorigenesis, we use human mammary epithelial cells (HMECs), combining various modes of E-cadherin suppression with other candidate oncogenic hits, to determine how E-cadherin inhibition or loss remodels the HMEC genome to facilitate ILC tumorigenesis. In RNA-seq of three independent HMEC models (HMEC lines 122, 153, and 184, with CCND1 over-expression), we found that antibody inhibition of E-cadherin and genetic suppression of E-cadherin by siRNA (siCDH1) and CRISPR/Cas9 knockout of CDH1 were strongly associated with signatures of epithelial-mesenchymal transition (EMT) and changes in lineage phenotype (i.e. luminal vs. basal). However, antibody inhibition and genetic suppression of E-cadherin had opposite effects, with antibody-induced lineage changes mirroring those seen in late tumor progression. These data support that genetic suppression of E-cadherin (modeling E-cadherin loss) is a distinct event establishing a unique molecular framework in ILC precursors. Gene set enrichment analysis showed that E-cadherin suppression repressed the EMT hallmark signature (NES= -1.66, -1.64, -1.60) ($q<0.01$). Notably, CDH1KO induced a phenotypic shift from basal progenitor to luminal progenitor, resembling the transcriptional phenotype seen in clinical ILC. Taken together, genetic suppression of E-cadherin shifts HMEC cells toward an ILC precursor phenotype, supporting E-cadherin loss remodeling the cellular transcriptome to facilitate ILC tumorigenesis.

14. **Differential interaction between mTOR and TFEB in oligodendrocytes by state of differentiation.** Packer, D; Macklin, WB.

    In oligodendrocytes, the cells responsible for central nervous system (CNS) myelination, the Transcription Factor EB (TFEB) regulates expression of pro-apoptotic genes. Disrupting TFEB activity in oligodendrocytes increases cell survival in normally unmyelinated parts of the CNS. Well-studied in non-oligodendroglial cells, TFEB regulates endolysosomal, autophagic, and apoptotic gene expression. Furthermore,

mammalian target of rapamycin (mTOR) signaling complex 1 (mTORC1) regulates TFEB nuclear localization, and thereby its transcriptional activity. mTORC1 senses nutrient availability and regulates numerous metabolically demanding cellular tasks including endolysosomal activities. Evidence supports differential activities of mTORC1 in oligodendrocytes of the brain versus those of the spinal cord. These differences may extend to TFEB as well. Endosome recycling and lysosomal activities are also involved in myelination. Despite their clear connection in non-oligodendroglial cells, mTOR, TFEB, and endolysosomes have not yet been studied as a single system in oligodendroglia. Objectives: (1) to elucidate interactions between mTOR, TFEB, and endolysosomes in oligodendrocytes of the brain and spinal cord and (2) to determine how the mTOR-endolysosomal-TFEB system affects oligodendrocyte survival, differentiation, and myelination. Methods: primary rat oligodendrocytes were differentiated for a set number of days in culture. Cells were then deprived of amino acids with or without the mTOR inhibitor, Torin. Oligodendrocytes were stained for lysosomes or for TFEB and imaged with a confocal microscope. Images were analyzed using blinded semi-automated processes. Results: in differentiated oligodendrocytes from both the brain and spinal cord, Torin treatment resulted in TFEB nuclear translocation. However, in immature oligodendrocytes from the brain, Torin treatment did not result in TFEB nuclear translocation. Amino acid deprivation alone was insufficient to cause TFEB nuclear translocation. TFEB protein expression transiently increased in oligodendrocytes with increasing differentiation, as found in previous studies by other investigators. Neither amino acid deprivation, nor Torin treatment yielded detectable changes in lysosomal quantity, intensity, or localization. Conclusion: while additional experiments are pending, the current results support an increasing role for mTOR in regulating TFEB activity in oligodendrocytes with increasing differentiation. Given that TFEB regulates transcription of pro-apoptotic genes, this may mean that oligodendrocytes are increasingly vulnerable to mTOR perturbations with increasing differentiation. Experiments in progress will determine the effects of mTOR disruption on TFEB in a myelinating co-culture system, and the effects of endolysosomal disruption on oligodendrocyte survival, differentiation and myelination.

15. **Alternative Splicing Derived Proteoforms Show Chamber-Biased Expression and Remodeling of Intrinsically Disordered Regions in Human Hearts.** Boomathi, Pandi; Stella, Brenman; Alexander, Black; Dominic C. M. Ng; Edward, Lau; Maggie P. Y. Lam.

    Alternative splicing (AS) contributes to the functional diversity of the genome by allowing multiple transcript variants to be encoded by one gene. Prior work using transcriptomics has shown that AS is highly tissue specific and has strong potential to alter protein interaction networks. In contrast, knowledge into the protein-level existence and function of the translated protein isoforms remain lagging. We and others have previously employed a proteogenomics approach that combines information from transcriptomics and proteomics to identify hundreds of AS-derived isoforms in mammalian tissues and cell lines. Here, we performed a computational analysis of mass spectrometry data to uncover AS-derived protein variants across chambers of the human heart.

Computational analysis by mining publically available mass spectrometry data sets in the human heart showed evidence for 216 non-canonical isoforms in the human heart atrium and ventricle, including 52 isoforms not documented on SwissProt and recovered using an RNA sequencing derived database. Among non-canonical isoforms, 29 show signs of regulation based on statistically significant preferences in tissue usage, including a ventricular enriched protein isoform of tensin-1 (TNS1) and an atrium-enriched PDZ and LIM Domain 3 (PDLIM3) isoform 2 (PDLIM3-2/ALP-H). Using recently developed deep learning based software tools, we further examined the function of the expressed protein isoforms. Variant regions that differ between alternative and canonical isoforms are highly enriched in intrinsically disordered regions (IDR), and over two-thirds of such regions are predicted to function in protein binding and/or RNA binding. Our analysis lends further credence to the notion that AS diversifies the proteome by rewiring IDRs, which are increasingly recognized to play important roles in the generation of biological function from protein sequences.

16. **Cysteine promotes glycation: Implications for protein aging.** Panja, S; Rankenberg, J; Michel, C; Cooksley, G; Glomb MA; Nagaraj RH.

    Advanced glycation end products (AGEs) are one of the major protein modifications that occur with aging. In this process, lysine and arginine residues in proteins are glycated after exposure to sugars and glyoxal molecules. To date, it has been considered that the formation of AGEs mainly depends on the concentrations of the amino groups in proteins and carbonyl compounds. However, our study provides compelling evidence that the formation of AGEs on lysine residues is significantly increased by the presence of proximal cysteine residues and the availability of free thiols. Recombinant human αA-crystallin (αAC) and αB-crystallin (αBC) were treated with glyoxal (GO) or methylglyoxal (MGO). We observed greater levels of the AGEs, Nε-carboxymethyllysine (CML) and Nε-carboxyethyllysine (CEL) in αAC compared to αBC. Specifically, K70 and K166 in αAC were found to be heavily carboxyalkylated, located close to C142. Reductively alkylated cysteine residues in αAC significantly decreased the accumulation of CML and CEL. Also, mutating cysteine residue at 142 to alanine reduced CML and CEL levels. Moreover, supplementation with glutathione or N-acetyl cysteine enhanced AGE accumulation in αBC. The introduction of a cysteine residue near a lysine residue in αBC and the mutation of cysteine to alanine in αAC validated the critical role of cysteine residues, emphasizing their importance in AGE formation. Results also showed that the formation of reactive hemithioacetal intermediate in cysteine residues plays a key role in forming these AGEs. These findings not only deepen our understanding of AGE formation in tissue proteins but also hold promise for developing innovative AGE inhibitors to mitigate age-associated diseases.

17. **Human Retinal Organoid Model of Photoreceptor Cell Death Amenable to Drug Screening for Retinal Degenerative Diseases.** Shama Parween, Anna C. Howell, Stefanie Varghese and M. Natalia Vergara.

    Purpose: In dry age-related macular degeneration (AMD), loss of retinal pigment epithelium cells in the macula results in irreversible damage to the overlying photoreceptor cells, leading to central vision loss. Therefore, potential treatments aim at preventing photoreceptor death. To contribute to this objective, it is crucial to establish

pathophysiologically relevant disease models for the evaluation of these therapeutic strategies. The purpose of this study is to develop a human induced pluripotent stem cell (hiPSC)-derived retinal organoid (RO) model of photoreceptor cell death that mimics aspects of AMD pathophysiology and that can be applied to therapeutic development. Since smoking is one of the main environmental factors associated with AMD, we have devised a strategy involving the treatment of human ROs with cigarette smoke extract (CSE). We validated this model by assessing its impact on oxidative stress, mitochondrial health, and cell death mechanisms, and we developed assays for the quantification of outcome measures in live ROs.

Approach: Two hiPSC lines were differentiated into ROs for 180 days to allow for the development of relatively mature photoreceptor cells. ROs were treated with different concentrations of CSE or vehicle control, and evaluated at 0, 6, 24, 48 and 72 hrs. Inflammation, cell death, and photoreceptor markers were analyzed by ELISA, immunofluorescence, confocal microscopy, and quantified using Fiji software. Mitochondrial health and oxidative damage were assessed in live ROs through JC1 and DHE assays and evaluated by 3D automated reporter quantification using a TECAN spark plate reader.

Results: Our results showed an increase in TUNEL staining as well as caspase-3 and caspase-8 activation in CSE-treated ROs compared to controls. Damage was mostly localized to photoreceptor cells and could be regulated by titration and timing. CSE treatment also increased ROS production and mitochondrial membrane depolarization.

Conclusions: We report the first human RO model that recapitulates aspects of AMD pathophysiology. The combination of this model with our quantitative outcome measures in live organoids constitutes a powerful paradigm for the evaluation of potential therapeutics for the preservation of photoreceptor health. This valuable tool will complement animal studies, accelerating the development of new treatments for patients suffering from vision loss due to dry AMD.

18. **Small neuron-derived extracellular vesicles from individuals with Down Syndrome propagate Alzheimer's disease pathology and affect behavior of trisomic Ts65Dn mice.** Saternos, H; Postdoc, Banh, J; Granhom, AC; PhD Ledreux, A, PhD.

Down Syndrome (DS) is the most common chromosomal disorder worldwide. Individuals with DS develop Alzheimer’s disease (AD) decades earlier than the general population, with accumulation of amyloid-β plaques and neurofibrillary tangles as well as glial activation. Research studies suggest that neurodegeneration in the locus coeruleus (LC) precedes all other neuronal loss, and that the it results in a significant decline in norepinephrine levels, which may contribute to initiating neuroinflammation. However, the consequences of early AD pathology in the LC to the spread of pathology has not been examined in DS. The main purpose of this study was to determine whether neuron-derived extracellular vesicles (NDEVs) from individuals with DS-AD can exacerbate AD pathology in the LC neurons and/or seed AD pathology into other areas. NDEVs carry pathological proteins such as pTau and Aβ that reflect the cells they originate from, and evidence suggest that they can spread toxic misfolded proteins from cell to cell, contributing to the propagation of the pathology to nearby brain areas. We injected NDEVs isolated from plasma of individuals with DS-AD into the LC of Ts65Dn mice and assayed for pathological and cognitive hallmarks 3 months after injection. Using the

novel object recognition task along with the double-H maze, we found that Ts65Dn mice injected with DS-AD NDEV performed on these 2 tasks compared to those injected with healthy control NDEVs. Using immunofluorescent techniques, we found alterations in glial morphology as well as indicators of neuronal distress and early AD pathology. These data not only suggest that EVs contribute to the spread of AD pathology but that pathology in the LC-NE is sufficient to trigger pathology in other brain regions, affecting behavior. This furthers our understanding of the biological mechanisms for AD in DS which can lead to better diagnostic and therapeutic strategies for both those with DS and the general population.

19. **Myelodysplatic Syndrome-Associated Splicesome Mutations' Impact on the Host Defense.** Schafer, J; Gurule, N.J; Harris, C; Alper, S.

    Myelodysplastic Syndrome (MDS) is a hematopoietic stem cell disorder that has the potential for progression to Acute Myeloid Leukemia (AML). MDS is characterized by somatic mutations in hematopoietic stem cells that disrupt the generation and function of mature myeloid cells. There are several risks associated with MDS including increased susceptibility to infection. Conserved somatically acquired mutations in components of the pre-mRNA splicing machinery are commonly found in MDS patients. In our lab, we have utilized mouse models expressing MDS-associated spliceosome mutations and found that the mutation U2AF1-S34F induces defective neutrophil migration to the peritoneum during infection, resulting in lack of control of infection. I am investigating both a second mouse model that expresses another RNA splicing mutation, SF3B1-K700E, and looking at genotyped human PBMCs from MDS patients to determine if this mechanism or other mechanisms of immunodeficiency are present across other MDS genotypes.

20. **Recognition of ASXL orthologs by the ET domain of BRD4.** Karthik Selvam; Tatiana G Kutateladze.

    Regulation of gene-expression in Chromatin depend on specific protein–protein interactions between a number of epigenetic regulators. Mutation of genes encoding epigenetic regulators often drive cancer and developmental disorders. ASXL1 mutations are mainly comprised of nonsense or frameshift mutations which result in a truncation of the protein, terminating before the C-terminal portion of the protein. Such mutations are significantly enriched in acute myeloid leukaemia and myelodysplastic syndrome. It has been reported that mutations in ASXL1 promote an interaction with BRD4 which is another central epigenetic regulator. BRD4 is one of the members of the bromodomain and extra-terminal domain containing protein family. Here we present structural and biophysical characterization of an epitope near common truncation breakpoints present in all three ASXL proteins that binds ET domain from BRD4. The studies show that the interactions are analogous to all three ASXL orthologs contain a functional ET domain-binding epitope.

21. **Flow Cytometric Analysis of Adipose-Derived Stromal Vascular Fraction Harvested Using Two Common Types of Liposuction Cannula from Different Donor Sites in Autologous Fat Graft Surgery.** Shams, AS; Postdoc, Surgery. Nikoumaram, BN, Associate Professor, Plastic Surgery. Zare, SZ, PhD, Cellular and Molecular Biology.

Lipoaspirates, enriched in stromal vascular fraction (SVF) cells, have demonstrated enhanced fat graft retention and improved outcomes in autologous fat graft surgeries (1). Over the last decade, several studies have evaluated the impact of different harvesting methods, cannula types, collection depots, isolation, and injection techniques on the SVF cell population; however, surgeons still debate the optimum outcome (2–4). This study aimed to assess the impact of the Tonnard cannula with 1mm elevated sharp microports designed for fat cropping, which makes it one of the most aggressive cannula types ever made, versus the Sorensen cannula with beveled microports, on the yield and viability of SVF cell populations in various donor harvesting sites. We sought to identify the most effective harvester and donor region to optimize SVF cell population.

Method: Lipoaspirates were harvested using Suction-Assisted Liposuction (SAL) at a negative pressure of 20 mmHg from 12 healthy donors undergoing autologous fat graft surgery. The Tonnard cannula was employed on the right side of the body, including the flank, inner thigh, and inner knee, whereas the Sorensen cannula was utilized on the left side. The diameter, length, and hole count of both cannulae were identical. Lipoaspirates were digested using the conventional enzymatic method, and the isolated stromal vascular fractions were analyzed by a Fluorescence-Activated Cell Sorting (FACS) Calibur Flow Cytometer device to assess the total cell yield, viability and apoptosis assays using Annexin V and propidium iodide (PI) staining, Reactive Oxygen Species (ROS) using DCFH-DA staining, and the expression of stem cell CD markers (CD105, CD73, CD90, CD45, and CD11b).

Result: The Tonnard cannula demonstrated a higher mean yield of viable SVF cells and positive CD markers ($P < .05$) irrespective of the suction region compared to the Sorensen cannula. Regardless of the cannula type, the flank area exhibited the highest concentration of viable cells.

Conclusion: Our results indicated that lipoaspirate extracted using the Tonnard cannula in the flank area provided the highest number of viable cells and mesenchymal stem cell CD marker expression. Further research endeavors will aim to enhance the robustness of this finding by utilizing a broader range of CD markers, performing gene expression analysis, assessing the functionality of the cells in vitro.

22. **NLRP3-induced contractile dysfunction in right ventricle cardiomyocytes is sexually dimorphic and modified by 17β-estradiol via estrogen receptor α.** Fais, R.S[1]; Kopf, K[1]; Hoffer, C.[2]; Walts, A.D,[1]; Cook, T.[3]; Fisher, A.K.[3]; Frump, A.L.; Woulfe, K.C.[2]; Pullamsetti, S.S[4]; Bonnet, S[5], Lahm, T[1, 2, 6].

[1] National Jewish Health, [2] University of Colorado, Division of Pulmonary Sciences and Critical Care Medicine, [3] Indiana University School of Medicine, [4] Max Planck Institute for Heart and Lung Research, [5] Université Laval, [6] Rocky Mountain Regional VA Medical Center

Introduction: NLRP3 inflammasome activation in macrophages promotes RV failure in pulmonary hypertension (PH). However, the role and regulation of NLRP3 signaling in RV cardiomyocytes (RVCMs) have not been studied. 17β-estradiol (E2) improves RVCM function in PH. We hypothesized that NLRP3 inflammasome activation mediates RVCM contractile dysfunction and that this is attenuated by E2 via estrogen receptor (ER) α. Methods: RNA-seq and proteomics were performed in RV tissues from control and PH patients with RV failure. RV failure was induced in male and female Sprague-Dawley rats with monocrotaline (MCT) or pulmonary artery banding (PAB). RVCMs isolated from healthy male or female wildtype (WT) or ERα loss-of-function mutant (ERαmut) rats were treated with NLRP3 activators lipopolysaccharide (LPS; 1 μg/mL, 4 h) and ATP (2 mM, 10 min) or endothelin-1 (ET-1; 10 nM, 4 h) in absence or presence of E2 (1 nM, 24 h) or NLRP3 inhibitor MCC950 (1 μM, 30 min). RVCM contractility was evaluated using the IONOPTIX system. Protein levels, immunolocalization and/or phosphorylation states of NLRP3, its targets, sarcoplasmic/endoplasmic reticulum Ca2+ transport ATPase 2 (SERCA2), mitochondrial calcium uniporter (MCU) and phospholamban were assessed. ERα binding to NLRP3 was assessed by co-immunoprecipitation. $P<0.05$ was considered significant. Results: RNA-seq and proteomics demonstrated upregulation of NLRP3 signaling in human RV failure. RVCMs from male, but not female, MCT- and PAB-rats demonstrated increased NLRP3-ASC co-localization, indicative of NLRP3 activation ($p<0.05$). Additionally, male MCT- and PAB rats RVs exhibited increased activation of NLRP3 downstream mediators caspase-1 and IL-1β ($p<0.05$). Cultured male RVCMs treated with LPS+ATP or ET-1 demonstrated more pronounced NLRP3 activation and contractile dysfunction than female RVCMs ($p<0.05$). E2 treatment in male WT RVCMs reduced NLRP3-ASC co-localization, increased contractility, and attenuated NLRP3-induced alterations in SERCA2 and MCU expression as well as phospholamban phosphorylation ($p<0.05$). E2's inhibitory effects on NLRP3 activation and NLRP3-induced contractile dysfunction in male WT RVCMs were abrogated in ERαmut RVCMs ($p<0.05$). Furthermore, in female RVCMs, resilience against NLRP3 activation and NLRP3-induced contractile dysfunction noted in the WT was lost in ERαmut RVCMs ($p<0.05$). ERα interacted directly with NLRP3. Conclusion: NLRP3 activation and NLRP3-induced contractile dysfunction in RVCMs are sexually dimorphic, with more pronounced activation and contractile dysfunction in males. ERα is required for E2 to prevent NLRP3-induced contractile dysfunction in male RVCMs and for female RVCMs to be protected against NLRP3-induced contractile dysfunction. Inhibiting NLRP3 by activating the E2-ERα-axis may be a novel treatment strategy for RV failure in males.

Acknowledgment: Pulmonary Hypertension Accelerated Bayer (PHAB) 3.0 award, NIH 5R01 HL144727-03, VA Merit Review Award 7I01 BX002042-09, and NIH 1P01 HL158507-01.

23. **Microglial Response to West Nile Virus Infection.** Teetsel, JFK; Clarke, P; Tyler, K.

    West Nile Virus (WNV) is a ssRNA flavivirus that is a leading cause of epidemic arboviral encephalitis. The virus enters the body by mosquito bite and multiplies in the local tissue before spreading through the body via the circulatory system. The virus is particularly deadly if it enters into the brain which can lead to neuronal cell death. Microglia are resident immune cells of the central nervous system that are capable of combating alterations to the CNS environment, like that caused by invasion by WNV. Microglia undergo a transformation of states from a quiescent state to a spectrum of reactive states once alterations to the normal neuronal environment are detected. In order to understand the timeline of microglial reactivity, transcripts were analyzed at various timepoints following disease induction. We identified a pattern of disease progression in the brain over a 14 day period that is first seen around 7 days following injection with WNV that starts with an interferon response and a microglial cell response. This continues onward as the brain begins to express inflammation genes to drive a general inflammation response. Microglia response 9 days following infection. This indicates WNV takes about 7 days to reach the brain following infection and infiltration initiates a microglial response within the brain.

24. **Investigations into Macrophage Polyamine Import.** Brian C. Tooker, PhD; Alexandra L. McCubbrey, PhD.

    Polyamines are small positively charged metabolites of arginine that have been linked to multiple cellular processes including cell proliferation, chromosomal accessibility, mRNA stability, and protein translation. While polyamines are generated by cells through sequential metabolic steps, they may also be imported from the extracellular surroundings. Our laboratory has previously shown that macrophages increase their intracellular polyamines utilizing a Rac1-dependent polyamine import pathway, following engulfment of apoptotic corpses. Rac1 is a Rho family GTPase that controls myosin II activity through phosphorylation, in effect controlling cellular contractility and endocytosis. How Rac1 activity is regulated, and whether it acts in concert with or independently from polyamine import channel proteins remain unknown.

    Rac1 dependency initially suggested the hypothesis that cellular polyamine import occurs via endocytosis and treating RAW264.7 macrophages with a Rac1 inhibitor (NSC23766) resulted in the same levels of import suppression across various cell culture media serum levels. However, RAW264.7 macrophages in serum free media were more sensitive to AMXT-1483, a polyamine channel blocker, than cells in media with 10 or 20% serum. These results suggest a revised hypothesis that macrophages have two independent polyamine import pathways: one specific for unbound polyamines and one more generalized for free and protein bound species. To expand upon these findings, mixtures of different inhibitors were utilized to target channel proteins (Trimer or AMXT-1483) or endocytosis (NSC23766, Dynasore, Cytochalasin or Wortmannin). Additive effects of channel and endocytosis inhibitor mixtures strengthen our multiple import pathway hypothesis. Both AMXT-1483 and Trimer have additive inhibitory effects when mixed with either NSC23766 or Wortmannin (PI3K inhibitor). Intriguingly, AMXT-1483 and not Trimer also has an additive inhibitory effect when mixed with dynasore (Dynamin inhibitor). Mixing Trimer, which inhibits the intracellular polyamine channel protein ATP13A2, with dynasore actually decreased the effectiveness of Trimer. These

results suggest that Trimer may be acting downstream of dynasore inhibited endocytosis while AMXT-1483 may be acting separately from the endocytosis.

It is quite clear that polyamine import is not a simple matter and may be confounded by the makeup of cell culture media. We have confirmed that polyamines bind cell culture media components, most likely proteins, in a pH dependent manner and this binding could affect how polyamines are imported by the cell. However, understanding the mechanisms of polyamine import is key to harnessing the therapeutic potential of polyamines to manipulate macrophage immune responses and a prerequisite for interpreting cell culture model results where the presence of serum in the media may alter the route of polyamine import or cellular availability.

25. **IL 18 maintains epithelial homeostasis by regulating the expression of antimicrobial peptides.** Zhantao Yu, Postdoc, CU Anschutz, Elena Reshetnikoff, PhD student, Rocky Vista University.

    Epithelial barrier dysfunction and crypt destruction are hallmarks of inflammatory bowel disease (IBD). Paneth cells (PC) residing in the crypts play a crucial role in antimicrobial peptides secretion. However, how PCs are dysregulated in IBD remains poorly understood. Here, we observe reduced IL18 protein levels in IBD patients, and mice with conditional IL18 depletion in the PCs (IL18ΔPC) exhibit an increased susceptibility to experimental colitis. Notably, IL18ΔPC mice display a significant reduction of antimicrobial peptides. Collectively, our findings highlight antimicrobial peptides reduction in PCs as a risk factor in IBD.

26. **Antibiotics used to treat Pseudomonas infections may enhance Mycobacterium abscessus persistence in the CF lung.** Corley J.M.; Congel, J.H., Haist, K.C.; Ochoa, A.E.; Malcom. K.C., Nick, J.A.; & Hisert, K.B.

    Background: Non-tuberculous mycobacterial (NTM) infections are increasing globally and infect a significant portion of people with cystic fibrosis (PwCF). Thus, a critical need exists to understand determinants of susceptibility to NTM. Co-infection with Pseudomonas aeruginosa has been found by some to be a risk factor associated with acquisition of NTM pulmonary infection in PwCF. NTM species like Mycobacterium abscessus (Mabsc) are resistant to antibiotics used to treat P. aeruginosa; thus, it is generally thought that these antibiotics do not affect NTM viability in the lung. Because previous work demonstrated that subinhibitory concentrations of the anti-Mabsc aminoglycoside amikacin activates expression of the transcription factor WhiB7 and increases survival of Mabsc in macrophages, we hypothesized that antibiotics with similar mechanisms of action used to kill P. aeruginosa would also induce whiB7 expression. Here we demonstrate that tobramycin, an aminoglycoside antibiotic (like amikacin) frequently administered to PwCF with P. aeruginosa during exacerbations and as a maintenance therapy, also activates whiB7 expression. As follows, we hypothesize that tobramycin used to kill P. aeruginosa in the CF airway enhances Mabsc persistence in macrophages by inducing whiB7 expression, thus increasing the chance of Mabsc becoming a chronic infection in the lung.

Methods: Gene expression of Mabsc whiB7 after tobramycin, amikacin, and levofloxacin treatment was measured using qRT-PCR. Growth of Mabsc wild type (wt) and whiB7 deletion strains (ΔwhiB7) were measured in human monocyte-derived macrophage (MDM) and alveolar macrophages (AlvMac) after 4 days. Reactive oxygen species (ROS) resistance of Mabsc +/- antibiotic treatment and ΔwhiB7 was evaluated using H2O2 MIC assays. To determine if tobramycin increased Mabsc persistence in vivo, mice were administered tobramycin one day prior and during infection with wt Mabsc and bacterial burden was assessed after 7 days of infection.

Results: We demonstrated that tobramycin-mediated induction of Mabsc whiB7 expression was dose dependent and temporal. Maximal expression of whiB7 occurred after 24-hour treatment with 25 mg/ml tobramycin. Induction of whiB7 did not occur with the fluoroquinolone levofloxacin, an oral antibiotic used to treat P. aeruginosa infections in PwCF. Treating Mabsc with amikacin prior to infection in both MDMs and AlvMacs promoted Mabsc survival and amikacin and tobramycin enhance resistance to H2O2. Furthermore, compared to wt, ΔwhiB7 Mabsc demonstrated decreased survival in macrophages and a lower H2O2 MIC. Treatment of mice with parenteral tobramycin resulted in increased lung Mabsc burden at 1 week as compared to placebo treated mice.

Conclusion: Our data suggest that tobramycin used to treat P. aeruginosa changes Mabsc gene expression to promote Mabsc survival in the host. Similar gene expression changes are not seen after exposure of Mabsc to levofloxacin, suggesting the antibiotic effects on Mabsc survival may be class specific. Future tobramycin treated Mabsc RNAseq studies will determine what WhiB7 regulated Mabsc genes are activated by tobramycin. We will also assess clinical relevance by evaluating whiB7 expression in clinical Mabsc isolates after tobramycin exposure by qRT-PCR studies. This study addresses mechanisms by which Mabsc infections may persist in some PwCF, and suggests that current antibiotic therapies for other CF pathogens may affect Mabsc infection.

27. **Advanced stage melanoma during pregnancy: real world management.** J.S.W. Borgers; D.B. Johnson; E. Livingstone; E.I. Buchbinder; W.A. Robinson; O. Hamid; M. Ferreira; F. Dimitriou; G.V. Long; P.A. Ascierto; A. Daletzakis; Y.G. Najjar; G.A.P. Hospers; J.S. Choi; F. Amant; K.K. Tsai; Z. Eroglu; J.B.A.G. Haanen; I.C. Glitza¬†

Treatment (tx) of advanced melanoma during pregnancy represents a major challenge. While management of early-stage melanoma is similar to non-pregnant patients (pts), very little data is available on outcome or tx guidelines for pregnant pts with advanced stage. Therefore, we collected real world management data, to ultimately develop management guidelines for these pts.

Methods:
This retrospective, international, multicenter database, included pts who either were diagnosed with advanced melanoma (newly diagnosed or recurrent) during pregnancy

(group 1) or conceived while on systemic tx for melanoma (group 2) between 01/2011,Äì06/2023. Patient, primary tumor and advanced melanoma characteristics, intervention/tx during pregnancy, and outcomes of mother and fetus were collected using a standardized, de-identified form.

Results:
68 pts from 7 countries were included, with a total of 72 pregnancies: 60 pregnancies in group 1 and 12 in group 2, including 5 twin pregnancies. Median age at time of pregnancy was 32 (19-42).

In group 1, advanced melanoma diagnosis occurred during the 1st trimester in 38%, followed by 3rd (32%), 2nd (22%) and unknown (8%) trimester. 2% had stage II melanoma, 48% stage III, and 50% stage IV. 76% were cutaneous melanoma, 7% mucosal, and 17% other subtypes. BRAF mutations were seen in 70%. Pregnancy was terminated in 15% of cases, and miscarriage occurred in 1 case. Of the 50 live births, 68% were induced and 56% were preterm (38% vaginal, 54% C-section). Median gestational age (MGA) was 34 wks (27-40). Systemic tx was initiated during pregnancy in 8 pts (targeted therapy [TT, 63%], immunotherapy [IT, 37%]). 90% switched or initiated new systemic tx after pregnancy (median time to start of therapy: 28 days; IT 65%, TT 27%, chemo 8%). 5-year overall survival (OS) was 49% (95%CI 34-69), with a median follow-up (MFU) of 26m.

In group 2, 82% had cutaneous melanoma and 18% an unknown primary. 91% had a BRAF mutation. 42% of pts received systemic tx for stage III melanoma and 58% for stage IV (IT 75%, TT 25%). 33% of pregnancies were terminated, 8% ended in miscarriage. Of the 8 live births, 43% were preterm, 29% were induced (43% vaginal, 29% C-section). MGA was 35 wks (32-39). Half the pts initiated new or continued tx after pregnancy (IT 50%, TT 50%). 5-year OS was 78% (95%CI 55-100), with MFU of 48m. Of the 57 live births, 1 child born at 26w died after 3 days. No children developed melanoma, despite 5 placentas with melanoma involvement. 4 unexposed children had congenital deficits: prematurity-related (n=3) and congenital hypothyroidism (n=1). 1 child with 3rd trimester Vemurafenib exposure had heart malformations, and 2 experienced toxicity after in utero IT exposure.

Conclusions:
This is the largest contemporary dataset of pts diagnosed with advanced melanoma during pregnancy and pts who became pregnant on systemic melanoma therapy, and provides a basis for developing clinical guidelines for this challenging population.

28. **Psychosocial Stressors in Young Mothers and Families: A Latent Class Analysis.**
Kim, B; Wolcott, C; Smith, H; Ashby, B.

INTRO

The Young Mothers and Families Clinic (YMFC) at Children’s Hospital Colorado (CHCO) is a dyadic parent-child medical home that provides integrated behavioral health (IBH) in pediatric primary care for both adolescent parents and their children. Understanding patterns of psychosocial stressors can support IBH efforts to promote well-being in adolescent parents and their infants.

METHODS

Screened for psychosocial stressors and postpartum depression (Edinburgh Postnatal Depression Scale) from families of infants 6 months old (54.2% Hispanic [all races], 15.1% non-Hispanic Black, 4.7% non-Hispanic White, 1.1% non-Hispanic Asian, 24.6% Unspecified; 96.4% Medicaid insured). Latent Class Analysis (LCA) in R Statistical Software (v4.3.2; R Core Team 2023) identified 2 latent classes (High and Low Stress).

RESULTS

Low Stress had few psychosocial needs. High Stress had concerns about meeting basic living costs (72.4%), food insecurity (48.3%), accessing benefits (44.8%), healthcare access (41.7%), and housing insecurity (13.8%). The High Stress group (M = 5.27, SD = 4.93) had significantly higher scores on the EPDS compared to the Low Stress group (M = 3.62, SD = 4.28), t(335) = -1.87, p = .03

DISCUSSION

Majority of the High Stress group reported difficulty meeting basic living costs. Examining psychosocial stressors and their relation to parental mental health may have meaningful implications for how IBH services can address family wellbeing holistically.

29. **The Use of Peripheral Blood Monocyte Cells (PBMC) to Improve Diagnosis for Specific Pathogens in Spinal Infections.** Maria Pogue, D.O.; Veronica M. Butler, B.S.; Gregory Ottenberg, Reed Ayers, PhD; Christopher Kleck, M.D.; David Ou-Yang, M.D.; Gowrishankar Muthukrishnan, PhD; Cheryl Ackert-Bicknell, PhD.

1. Department of Orthopedics, School of Medicine, University of Colorado, Aurora Colorado.
2. Colorado Program for Musculoskeletal Research, University of Colorado, Aurora, Colorado.
3. Center for Musculoskeletal Research, University of Rochester, Rochester, NY

Post-operative spinal infections are associated with high rates of morbidity and mortality. Post-operative infections are monitored by fever, pain, neurological changes, and serum inflammatory markers (CRP and ESR). The long-term goal of this study is to develop between diagnostic markers to monitor post-operative infections. We collected whole blood samples from patient undergoing known spinal hardware revision surgery. PMBCs were isolated, washed, and cells were removed and counted. WBC fractions were analyzed at baseline, two weeks, six weeks, three months, and six months. WBC fractions were not different at baseline between infected and non-infected patients. Using linear discriminate analysis, PBMS numbers had a better infection type than classical clinical variables.

30. **Engineered nanomedicines for targeting and promoting pancreatic β-cell survival during the onset of type 1 diabetes.** Akolade, J; Collins, J; Fremin, A; Farnsworth, N.

    Clinical interventions to prevent pancreatic β-cell stress or death during type 1 diabetes (T1D) onset are promising curative strategies that could halt or reverse the disease progression. The pathogenesis of T1D at the very early stage involves pro-inflammatory cytokines contributing to the immune destruction of pancreatic β-cell and islet dysfunction. Previous studies have shown that protein kinase C δ (PKCδ) partly mediates cytokine-induced apoptosis of the pancreatic β-cell and δV1-1, a specific inhibitor of PKCδ activation, protects against cytokine-induced death in isolated islets. However, peptide-based drugs are characterised by poor bioavailability and non-linear pharmacokinetics. We hypothesise that δV1-1 nanocapsules (NCs) functionalised with targeting peptides can precisely deliver the PKCδ inhibitor to pancreatic β-cell in vivo, preventing cell death and promoting survival and function. Model cargoes (Cy5 and pentamidine) or δV1-1 were encapsulated in polycaprolactone NCs and coated with either glucagon-like peptide-1 receptor agonist Exendin-4 conjugated to hyaluronic acid (HA-Ex4) for specific β-cell targeting. The coated NCs were characterised and evaluated in vitro using isolated mouse and human cadaveric islets treated with or without cytokines and in vivo with NOD mice. Our results showed that coatings of nanocapsules with the targeting peptide facilitate selective uptake of the Cy5 by the pancreatic β-cells in both in vitro and in vivo models. Data from the in vivo pentamidine model also showed that in vivo modulation of pancreatic β-cell was concentration-dependent in tandem with in vitro experiments. Encapsulation of δV1-1 in the nanocapsules does not affect its effectiveness in protecting pancreatic cells against cytokine-induced death when compared to the action of free δV1-1. These findings suggest that targeted delivery of δV1-1 using this approach could enhance its therapeutic potential and warrants further investigation in mouse models of T1D onset.

31. **Using Eye-Tracking and Pupillometry to Understand the Impact of Auditory and Visual Noise on Speech Perception.** Alzoubi, H; Postdoc.

    Although speech recognition is often experienced as relatively effortless, there are a number of common challenges that can make speech perception more difficult and may greatly impact speech intelligibility (e.g., environmental noise). However, there is some indication that visual cues can be also used to improve speech recognition (Baratchu et al., 2008) — especially when the visual information is congruent with the speech signal (e.g., talking faces; Massaro, 2002). However, it is less clear how noisy visual environments may impact speech perception when the visual signal is not congruous with the speech signal. In fact, adding incongruous visual information will likely detract precious cognitive resources away from the auditory process, making speech perception in noise a more cognitively difficult task. Therefore, the purpose of this dissertation was to examine cognitive processing effort by measuring changes in pupillary response during the processing of speech in noise paired with incongruous visual noise. The primary hypothesis was that noisy visual information would negatively impact the processing of speech in noisy environments and that would result in a greater pupil diameter. To test this I used a common eye-tracking measure (i.e., pupillometry) to

assess the cognitive processing effort needed to process speech in the presence of congruent and incongruous visual noise. The results indicated that visual noise recruits cognitive processing effort away from the auditory signal. Results also indicated that different combinations of auditory and visual noise have a significant impact on cognitive processing effort, which led to an increase in pupil dilation response during speech perception.

32. **Pulmonary viral infection promotes the awakening of dormant metastatic breast cancer cells in lungs.** Chia, SB*; Johnson, BJ*; Boorgula, M; Sreekanth, V; Goodspeed, A; Davenport, BJ; Hu, J; Gao, D; Papanicolaou, M; Morrison, TE; Aguirre-Ghiso, JA; Rincon, M; DeGregori, J.

    Background: Breast cancer is the most common form of cancer and the second cancer-causing death in females. Although remission rates are high if detected early, survival rates drop substantially when breast cancer becomes metastatic. The most common sites of metastatic breast cancer are bone, liver, and lung. Respiratory viral infections inflict illnesses on countless people, as evidenced by annual flu seasons and the latest pandemic caused by SARS-CoV-2. Respiratory viral infections result in increased inflammation with immune cell influx to facilitate viral clearance. Prior studies have shown that inflammation can contribute to dormant cancer cells awakening and outgrowth. However, how respiratory viral infections contribute to breast cancer lung metastasis remains to be unraveled.

    Methods: MMTV/NEU mouse model of dormant breast cancer was used, with influenza virus as the model respiratory virus. Lungs and bronchoalveolar lavage fluid were harvested for immunohistochemistry, flow cytometry, cytokines, and single-cell RNA-seq analysis. Flatiron Health Database was mined for epidemiological data to assess the risk of breast cancer metastasis to lung with COVID infection.

    Results: We have shown a dramatic increase in disseminated cancer cell (DCC) awakening in the lungs following influenza and SARS-CoV-2 infections. Influenza infection results in loss of a pro-dormancy mesenchymal phenotype and increased proliferation of DCC in the lungs within days post-infection, with a more than 1000-fold expansion of carcinoma cells over a couple of weeks. Strikingly, by 15 days post-infection, the lesions that expanded from solitary HER2+ DCCs almost homogeneously return to a quiescent state. Our preliminary data indicate that post-infection increases in IL-6 are required for DCC expansion post-influenza. Acute influenza infection also contributed to an accumulation of CD4+ T cells around expanding tumor cells for as long as 28 days after the initial infection. Depletion of CD4+ T cells but not CD8+ cells during infection with influenza virus prevents the expansion of the DCCs in the lung. Co-depletion of CD8 cells with CD4 cells partially restored the DCC burden in the lungs, indicating a role for CD8 cells in eliminating DCCs when released from CD4-mediated suppression. Single-cell RNA-seq analyses of CD8+ T cells with CD4 depletion showed an increased IL2/STAT5, MTORC1, and Ox/Phos activation by 15 dpi. The analyses also showed an immunosuppressive effect by the tumor cells. Finally, analysis of female

breast cancer patients who tested positive with SARS-CoV-2 after their initial diagnosis exhibited a hazard ratio of 1.44 (p=0.043) for subsequent diagnosis of metastatic breast cancer in lungs.

Conclusions: These studies reveal the potential risks to cancer survivors who experience respiratory viral infections, with mechanistic insight that could lead to novel prevention or intervention strategies.

33. **4D flow MRI hemodynamic quantification of pediatric patients with multi-site, multi-vendor, and multi-channel machine learning 3D segmentation.** Takashi Fujiwara; Haben Berhane; Mike Scott; Erin Englund; Michal Schäfer; Brian Fonseca; Alexander Berthusen; Joshua Robinson; Cynthia Rigsby; Lorna Browne; Michael Markl; Alex J Barker.

Background
Blood flow velocity in the heart and blood vessels can be measured by a magnetic resonance imaging (MRI) technique called 4D flow (3D + time) MRI. 4D flow is a promising imaging technique particularly for pediatric patients with complex congenital heart disease (heart defects that are present at birth) because it can measure time-resolved, three-dimensional blood flow at any position of the heart with a single MRI scan. To measure blood flow velocity using 4D flow, accurate blood vessel segmentation (extraction of target blood vessels from the 4D flow image) is necessary, but manual segmentation takes 30-60 minutes. Recently a deep learning-based automated segmentation has successfully reduced processing time for adult 4D flow data. However, its performance has not been investigated for pediatric patients with congenital heart disease. Due to large variability in the cardiac anatomy of congenital heart disease patients, data from a single site may not be sufficient to achieve excellent performance.

Aim
To establish a fully automated pipeline to segment the aorta and pulmonary arteries for pediatric patients' 4D flow MRI using a deep learning network trained on multi-site 4D flow data.

Hypothesis
The deep learning network trained on multi-site 4D flow data will outperform the one trained on single-site data and shorten the long processing time for segmentation.

Methods
Cardiac 4D flow data of volunteers and pediatric patients were retrospectively collected from Children's Hospital Colorado (Aurora, CO; site 1; n=100) and Lurie Children's Hospital (Chicago, IL; site 2; n=74). A deep learning network called dense U-net was trained on data from each single site (single-site networks) and from both sites (multi-site network). 10-fold cross validations were used to compare segmentation performance between single- and multi-site networks. Performance metrics include Dice scores (geometrical similarity between manual and auto segmentations for the aorta and pulmonary arteries) and net flows measured at the ascending aorta and main pulmonary artery. $P<0.05$ was considered statistically significant.

Results

The median processing time for the auto segmentation was 1.01 seconds. No significant difference was found in Dice scores both for site 1 (median dice score for the aorta: single site 0.916 vs. multi-site 0.915, P=0.55; for pulmonary arteries: 0.894 vs. 0.895, P=0.64) and site 2 (for the aorta: 0.906 vs. 0.904, P=0.69; for pulmonary arteries: 0.870 vs. 0.869, P=0.96) data. Net flow quantified at the aorta and main pulmonary arteries were also not significantly different (P=0.75 for the aorta; P>0.99 for the pulmonary arteries). Although not statistically significant, visual inspection found the multi-site network improved segmentations for patients with congenital heart disease.

Conclusion
Segmentation based on the multi-site network is feasible for pediatric 4D flow MRI with a short processing time. Although no significant improvement was seen, the multi-site network maintained the performance of single-site networks. This deep learning pipeline will facilitate the clinical use of 4D flow for pediatric patients.

34. **Developing a Telenovela (Soap opera) to improve Self-management among Latinos with HIV.** Iriarte, E., Villegas, N., Cook, P., Stonbraker, S., Cianelli., R., Baeza, M.J, Toledo, C., Burk-Leaver, E., Sepulveda C., & Jankowski, C.

Purposes/Aims: To develop a culturally tailored telenovela (soap opera) for HIV self-management among Latinos living with HIV (LWH).
Rationale/Conceptual Basis/Background: As advances in treatment have transformed HIV from an acute to a chronic disease and people are living longer with HIV, effective HIV self-management interventions are essential. LWH need to self-manage their course of treatment, including maintaining ART adherence, physical health, psychosocial functioning, and daily adaptations to living with a stigmatized chronic illness. An identified gap in LWH care is the need for culturally adapted interventions to improve HIV self-management. A culturally tailored telenovela (soap opera) for HIV self-management is one strategy to fill this gap. Telenovelas are appealing and familiar to Latinos and have effectively reduced risky sexual behaviors among Latinos in South Florida and California. However, to our knowledge, there are no existing telenovelas that promote HIV self-management among LWH.
Methods: This study employs basic and formative research informed by the social cognitive theory (SCT), narrative engagement theory (NET), and research on emotional responses as action-guiding intervention delivery mechanisms. Thirty-two Spanish speaking aged ≥ 18 in Denver, CO, will be recruited. Telenovela vignettes will be co-created in Spanish in collaboration with a CAB (n=6), an expert panel (research team and consultant), and a telenovela director/producer. Contextual and cultural aspects will be incorporated into the telenovela stories. Then, we will explore the acceptability of the telenovela vignettes and assess strategies to effectively deliver the telenovela to target participants using focus groups conducted with LWH (n=24). Professional actors will video-perform the vignettes that will be presented to LWH. Additionally, participants will be characterized based on their demographics and health history and will complete questionnaires assessing acceptability and modality. Descriptive statistics and conventional content analysis will be used for the quantitative and qualitative data, respectively. This study is a partnership between the University of Colorado College of Nursing and the Colorado Health Network (CHN).
Assessment of Findings/Outcomes Achieved: Data collection is currently in progress. After conducting the study activities, a culturally relevant HIV self-management telenovela for LWH will be produced and filmed in Spanish based on the assertion that

LWH will identify with the telenovela content in a way that increases attention and comprehension.
Conclusions/Implications that emphasize next steps and recommendations for future undertakings: Upon conclusion of this study, we will have a filmed telenovela for HIV self-management among LWH. The study will help to improve the self-management behaviors of LWH by co-creating an easily accessible, culturally tailored, and linguistically appropriate HIV self-management educational tool. This study has the potential for major national public health significance, including the potential to impact HIV self-management and a wide array of health outcomes in this at-risk yet understudied population. By tailoring this telenovela to LWH needs, we will contribute to reducing barriers to adverse health outcomes related to HIV self-management and secondary HIV preventive outcomes. Based on these findings, we will be well-positioned to lead future studies to test the feasibility and acceptability of the telenovela for HIV self-management.

35. **Good agreement of turbulent kinetic energy assessment by compressed sensing-accelerated 4D flow MRI in aortic stenosis patients.** Park, S.; Jin, N.; Han, D.; Lee, B.Y.; Kwon, M.; Yi, J.-E.; and Huh, H.

    Introduction: Time-resolved three-dimensional phase-contrast MRI (4D flow MRI) has become a promising tool for complex hemodynamic analysis. Estimating TKE by 4D flow MRI can provide valuable information on flow energy dissipation within the aorta—beyond the capabilities of current echocardiography methods1. However, TKE estimation achieves high accuracy at a relatively low velocity-encoding (VENC) values2, indicating that additional MR scans are crucially required to obtain appropriate velocity information without aliasing. This potentially extends the scan time and hinders the practical clinical application of TKE estimation.

    Compressed sensing (CS) acceleration in MRI imaging has emerging as a promising method for reducing MR scan time of 4D flow MRI by only 2 minutes3. In addition, the reliability of CS-accelerated 4D flow MRI has been validated by comparing various hemodynamic parameters, including peak velocity, peak flow rate and wall shear stress, with conventional 4D flow MRI4. Although the applicability of CS 4D flow MRI has been extensively established, no studies have investigated the effect of CS acceleration on TKE estimation. Thus, this study aims to validate TKE using CS 4D flow MRI compared to TKE obtained by 4D flow MRI.

    Methods: A coarctation phantom model was used to validate TKE estimation between CS-accelerated 4D flow MRI (R=7.7) and conventional 4D flow MRI (GRAPPA, R=2) using in-house pulsatile pump. The 4D flow scans were performed on a 3T MRI system (MAGNETOM Skyra, Siemens Healthcare, Erlangen, Germany) at the Daegu Gyeongbuk Medical Innovation Foundation (KMEDIhub). Asymmetric VENC values of 200 and 300 (V200 and V300, respectively) were used to obtain TKE parameters, and symmetric VENC value of 400 was used to obtain appropriate velocity data. The sequence parameters were matched for both conventional and CS 4D flow scans as follows: TE/TR = 2.32–2.55/37.3–40.8, BW = 495–560 Hz/voxel, flip angle = 15°, spatial

resolution = 222 mm3, temporal resolution = 41.4–41.6 ms, cardiac time frames = 25.

To validate clinical applicability, 4D flow MRI images were acquired on two different 3T MRI systems: the Skyra (Siemens Healthcare) at the KMEDIhub for healthy subjects and the Vida (Siemens Healthcare) at Eunpyeong St. Mary's Hospital for AS patients. Demographics and MR scan parameters were summarized in Table 1. A two-tailed paired t-test was employed to evaluate statistical differences for TKE parameters. Bland-Altman analysis was also conducted to compare similarity between conventional and CS 4D flow. Change for CS [%] for TKE parameters was defined as the ratio of (CS 4D flow – Conventional 4D flow) to (Conventional 4D flow).

Results: The representative distribution of TKE in the in vitro model during peak systole is shown in Fig. 1. The peak location was similar between conventional and CS 4D flow at each VENC, but both peak location and TKE distribution varied depending on the VENC values. TKE estimation at V200 showed similar trends in TKEmax distribution (Fig. 1C), while both TKEmax and total TKE remained comparable even at V300 (Fig. 1D). In addition, both TKEmax and total TKE were similar especially at the low VENC and peak systole (Table 2). Fig. 2 illustrates the representative TKE distribution for both healthy subject and AS patient at peak systole. Healthy subject exhibited the higher number of elevated TKE in CS 4D flow (Fig. 2A,B). In contrast, TKE distribution appeared nearly identical between conventional and CS 4D flow in AS patient (Fig. 2C,D). Fig. 3 showed averaged TKE parameters for all healthy subjects and AS patients. AS patients had good agreement in TKE assessment between conventional and CS 4D flow with fewer or no significant differences.

Discussion: Our in vitro study demonstrated that VENC value plays an important role to minimize TKE bias, recommending to select VENC values ranging from 30% to 60% of the maximum velocity to achieve high accuracy of TKE5. In addition, TKE by CS 4D flow was overestimated in healthy subject especially at close to the ascending aorta. Spatial acceleration by the movement of the aorta significantly increases close to the vessel wall, which overestimates CS-accelerated TKE6. On the contrary, our in vitro and AS patient's cohort studies demonstrate that TKE estimation by CS 4D flow had good agreement with conventional 4D flow during systole where high flow regime potentially occurs. Thus, this suggests that TKE estimation could be a potential biomarker to estimate energy dissipation by AS severity. A detailed examination of the effect of acceleration factors and voxel size on TKE estimation will be further required for the practical clinical application.

Conclusion: CS 4D flow MRI demonstrated goodagreement in TKE estimation for AS patients, while healthy subjects showed significant differences.

Acknowledgements: This research was supported by the Basic Science Research Program through the National Research Foundation of Korea (NRF), funded by the Ministry of Education (NRF-2021R1C1C1003481); by Korea Health Technology R&D

Project through the Korea Health Industry Development Institute (KHIDI), funded by the Ministry of Health & Welfare, Republic of Korea (Grant Number: HI22C1915); and by the Korean Cardiac Research Foundation (202002-01).

36. **Distinguished serum protein patterns between heart failure and recovered patients provide insights into pediatric dilated cardiomyopathy as a single disease.** Vicentino, ARR; Karimpour-Fard, A; Stauffer, BL; Lipshultz, SE; Miyamoto, SD; Lavine, K.J; Sucharov, CC.

    Introduction: Pediatric cardiomyopathies, though rare, significantly contribute to morbidity and mortality in children. Dilated cardiomyopathy (DCM) is the most prevalent form and common reason for transplant in children over 1 year of age. While children with DCM have higher cardiac recovery rates, it is not possible to predict outcomes when these patients present with acute heart failure (HF).
    Hypothesis: We hypothesize that serum-circulating proteins from pediatric DCM patients can predict disease outcomes.
    Methods: Serum protein profiles were assessed using the SOMAscan proteomic assay. Samples were collected from children with DCM under 18 years of age at the time of presentation for acute HF or from age-matched non-failing (NF) controls. The primary outcomes, determined one year after enrollment or at the time the outcome was met, were transplant/mechanical circulatory support/death (n=31) or recovery (n=17). Welch's t-test with an adjusted FDR of $q<0.1$ was used to identify significantly dysregulated proteins. Ingenuity Pathway Analysis (IPA) was used to investigate predicted changes in biological pathways.
    Results: Circulating proteins can predict disease outcomes and differentiate patients who recovered from patients who had a poor outcome (Area Under the Curve=0.9). Core analysis by IPA identified 86 dysregulated molecules in the transplant group compared to NF controls: 10 downregulated and 76 upregulated. In the recovered group, 25 proteins were downregulated and 51 were upregulated. Pathway analysis suggests outcomes-specific biological processes.
    Conclusion: These findings suggest that distinct serum protein profiles are essential for understanding pediatric DCM pathogenesis. This could improve biomarker selection to predict outcomes in this population.
    Keywords: pediatric cardiomyopathy, biomarker, pathways

37. **Investigating the Role of TNF Signaling in Prevotella-Induced Airway Clearance of Streptococcus pneumoniae.** Stoner, SN, PhD; Fulte, SJ; Shaw, SC; Clark, SE, PhD.

    Streptococcus pneumoniae is a leading cause of death in children under five years of age and causes approximately 5 million cases of community-acquired pneumonia per year in the United States. While pneumococcal vaccines are effective against invasive disease, better therapeutics are still needed for protection against pneumococcal pneumonia. Studies suggest that the airway microbiome is protective against bacterial respiratory infections, including S. pneumoniae. Prevotella species commonly reside

within the upper airway microbiome, and increased abundance is associated with airway health and decreased S. pneumoniae. Previous work from our lab demonstrated that administering Prevotella melaninogenica to the lungs 24 hours before S. pneumoniae infection induces rapid S. pneumoniae clearance from the airways. This clearance is dependent on neutrophils, which also had a significant increase in TNF-a production after exposure to P. melaninogenica. However, the initial stages of myeloid cell recruitment after P. melaninogenica exposure remain unclear, as well as whether TNF-a signaling plays a role in enhanced killing of S. pneumoniae after P. melaninogenica exposure. In this study, we observed neutrophil recruitment starting 6 hours after P. melaninogenica exposure, as well as an inflammatory cytokine response dominated by TNF-a as early as 2 hours post-exposure. TNF-deficient mice (tnf-/-) showed reduced neutrophil recruitment to the lungs compared to wildtype mice after P. melaninogenica exposure. Additionally, neutrophils isolated from tnf-/- mice had reduced ability to uptake S. pneumoniae, while TNF receptor-deficient (tnfr1-/-) neutrophils had similar uptake capacity as wildtype neutrophils. This suggests that intrinsic neutrophil TNF-a production, but not exogenous TNF-a sensing, is required for enhanced S. pneumoniae uptake by neutrophils post- exposure. Taken together, these findings suggest an important role for TNF-a in Prevotella-induced neutrophil recruitment and uptake of S. pneumoniae.

38. **Can optogenetic stimulation of olfactory inputs alleviate Alzheimer's Disease progression?** Villanueva, J.A.; Postdoc, Departments of Neurology and Cell & Developmental Biology; Fillingim, S.; Research Associate, Cell & Developmental Biology; Niemeyer C.S.; Assistant Professor, Department of Neurology; A.N Bubak; Assistant Research Professor, Department of Neurology; Nagel, M.A.; MD Research Professor, Departments of Neurology and Ophthalmology; Restrepo D.; Professor, Department of Cell & Developmental Biology

    Alzheimer’s disease (AD) brain pathology includes deposition of β-amyloid (Aβ) plaques, phosphorylated-tau, neurofibrillary tangles, and microglial activation that lead to reduced gamma oscillation power and cognitive impairment (Murty D., 2021). Indeed, multi-sensory stimulation at 40 Hz reduces amyloid burden and increases microglial co-localization with Aβ (Iaccarino, HF., 2016). Loss of smell has emerged as an early feature of AD where decreased smell is linked to faster brain volume loss and cognitive decline (Murphy, C., 2019). Further, sniff-induced gamma oscillations from the olfactory bulb (OB) to the hippocampus suggest that loss of smell decreases hippocampal gamma oscillations. I hypothesize that stimulation of the OB in gamma frequencies will ameliorate AD pathologies by recruiting CD4+ T-cells and shifting microglia to a non-disease like states as well as improve learning and memory in a familial AD mouse model. I present optogenetic studies using OMP-hChR2V mice to stimulate olfactory sensory neurons and entrain the hippocampus in gamma oscillations. LFP recordings in the OB and dorsal CA1 show robust coupling to CA1. In a chemogenetic approach, I express the excitatory DREADD receptor, hM3Dq in CaMKIIa mice granule cells to enhance synchronous gamma firing (Dalal and Haddad, 2022). Oscillatory power changes were dose-dependent of the hM3Dq ligand, clozapine-N-oxide. At a high dose, there was a CA1 gamma power decrease, while at a medium dose, a transient increase followed by a decrease in gamma power in CA1 was observed. These findings

contribute to the understanding of the therapeutic effects of gamma frequency stimulation on AD pathology via an intranasal route.
Funded by an NIA administrative supplement to R01 DC000566, R01 AG079193 and T32 DC012280

39. **Women with HIV: The Dynamics of their M. tuberculosis-specific Innate and Adaptive Immune Responses during Pregnancy and Postpartum.** Yengkhom, D; Jalbert, E; Weinberg, A; and IMPAACT P1078 study team.

Background. Active tuberculosis infection (ATBI) predominantly affects young adults, including women of reproductive age. Pregnancy is associated with immune suppression due to the expansion of regulatory T cells, which prevent rejection of the allogeneic fetus. TB-specific Th1 responses measured by interferon ÔÅß release assay (IGRA) decreases in pregnant people with and without HIV. Th1 together with Th17 responses, are considered protective against ATBI. Interestingly, the incidence and morbidity of ATBI does not increase during pregnancy. This study investigates TB-specific Th1/Th17 and memory-like innate immune responses (trained immunity), which might contribute to protection against ATBI in pregnancy, in pregnant people with HIV (PPHIV). The study also evaluates the effect of isoniazid preventive therapy (IPT) on conventional T cell (Tconv) memory and trained immunity in PPHIV.
Methods. IGRA (+) PPHIV who participated in a randomized, double-blind, placebo-controlled study comparing 28 weeks of IPT initiated during pregnancy versus 12 weeks postpartum are included in this study. Cryopreserved peripheral blood mononuclear cells (PBMCs) are evaluated for TB-specific trained immunity and Th1 and Th17 responses using high-dimensional flow cytometry and single cell RNA sequencing (scRNA-seq).
Study Progress/Development. This study measures Tconv, natural killer cells (NK), natural killer T-cells (NKT), invariant natural killer T-cells (iNKT,) mucosal-associated invariant T-cells (MAIT), gamma delta T-cells ($\gamma\delta$ T-cells), conventional type 1 and 2 dendritic cells (cDC1 and cDC2), plasmacytoid dendritic cells (pDC), inflammatory DC (infDC) and monocyte cytokine production and expression of activation markers in response to ex vivo stimulation with M. tuberculosis antigens. We developed and optimized a 16-color multidimensional flow cytometry panel. To ensure quality of our data we established rigorous quality control and inter-batch normalization to avoid introducing experimental biases. To evaluate the transcriptomic profile, we are using fixed scRNA-Seq. We are multiplexing the fixed scRNA-Seq for the first time. To optimize the assay, we extensively experimented with cell hashing in different conditions and submitting the antibody-hashed cells to freezing and thawing.
Conclusion. At the current stage of this study, we streamlined the multidimensional flow cytometry quality control and normalization, and standardized cell hashing for fixed scRNA-Seq.
Keywords. tuberculosis infection, pregnancy, trained immunity, Th1, Th17, HIV infection, isoniazid preventive therapy.

40. **PREMENOPAUSAL WOMEN WITH NIGHTMARES RELATED TO POSTTRAUMATIC STRESS DISORDER HAVE EVIDENCE OF PREMATURE VASCULAR AGING.** ROSENBERRY, R; Cox, C; Schauer, I; DuBose, L; Holliday, R; McCarthy, M; Moreau, M.

INTRODUCTION: Posttraumatic stress disorder (PTSD) is a debilitating condition that disproportionately affects women. PTSD represents a form of persistent life stress that is

associated with premature cardiovascular disease (CVD) in women for reasons that remain unclear. Individuals with PTSD exhibit endothelial dysfunction, a key characteristic of vascular aging and an established precursor to CVD. Poor sleep quality due to frequent disturbances— a hallmark symptom of PTSD— is associated with systemic inflammation and accumulation of reactive oxygen species (ROS), key mediators of vascular aging. Accordingly, we hypothesized that premenopausal women with nightmares and poor sleep quality related to PTSD would display evidence of premature vascular aging. METHODS: Premenopausal women (N=13, 30±8 years) with PTSD-related nightmares and poor sleep quality (Pittsburgh Sleep Quality Index [PSQI] >6) were compared with premenopausal and postmenopausal women controls who reported no distressing dreams or poor sleep quality. Measurements of sleep quality (PSQI), and endothelial function (brachial artery flow-mediated dilation [FMD]) were performed in all women. RESULTS: Sleep quality was worse in premenopausal women with PTSD-related nightmares (PSQI 12.2±5.1, $p<0.001$) than premenopausal (PSQI 4.2±3.1) and postmenopausal (PSQI 2.8±2.4, $p<0.001$) controls. Brachial artery FMD was lower in premenopausal women with PTSD compared with premenopausal women (7.8±2.9% vs. 11.3±4.5%, $p=0.031$) controls. FMD was lower in postmenopausal (5.3±1.7%, $p<0.025$) compared to both premenopausal groups. CONCLUSIONS: These data support the hypothesis that premenopausal women with PTSD-related nightmares and poor sleep quality exhibit premature vascular aging relative to premenopausal controls. Future studies are needed to determine whether interventions focused on addressing sleep- and nightmare-related sequelae can mitigate the effects of chronic sleep disturbances on vascular aging and CVD risk.

41. **Progenitor Cell Proliferation versus Differentiation during Premalignancy of Lung Adenocarcinoma**. Khosbayar Lkhagvadorj; Postdoc, Alexis Assante; BS, Melissa L New; MD, Amy B Frey; MD, Simran Randhawa; MD, Robert L Keith; MD, York E Miller; MD, and Moumita Ghosh; PhD.

    Introduction: Lung cancer is the leading cause of cancer deaths with a poor 5-year survival. Interventions during premalignancy can improve outcomes. Epithelial progenitors are critical cells that maintain and repair the airways due to their abilities for proliferation and differentiation. Using 3D organoid cultures we have found diminished progenitor function in the premalignant field that contained lung adenocarcinoma (ADC). In the current study, we tested whether progenitor dysfunction involves loss of proliferation and/or differentiation.

    Methods: Lung tissues resected for early-stage lung ADC (n=12) were used. To study progenitors in premalignancy, lung organoids were grown from tissues collected from the uninvolved (UN) (5 - 15 cm) and tumor-adjacent (TA) (0.2 - 2 cm) from the surgical margin. EpCAM+ epithelial cells were isolated, and organoids were cultured under either proliferation or differentiation conditions. Molecular profiles of organoids were examined by single-cell RNA-sequencing (ScRNAseq).

    Result: We found an opposing outcome of proliferation and differentiation function of progenitor cells from the UN and TA tissues. Under proliferation conditions, significantly greater numbers of organoids were made by tissues from the TA, while under

differentiation conditions, UN areas gave rise to greater numbers of organoids ($p<0.05$ both). Immunostaining and quantification revealed higher numbers of proliferative (Ki67+) basal cells (KRT5+) in TA organoids under proliferation, while no difference was detected under differentiation conditions. ScRNAseq annotation identified a specific basal cell cluster in organoids from TA tissues that was enriched for genes belonging to EGFR signaling with higher expression of amphiregulin (AREG), a canonical ligand for EGFR. Immunostaining was used to confirm the presence of AREG+ cells in organoids from the TA tissues and not in the organoids from the UN.

Conclusions: Our results indicate that progenitors within TA tissue are highly proliferative, and less differentiating, compared to UN tissues and this phenotype could be driven by AREG-mediated signaling.

Sponsors


Colorado Clinical and Translational Sciences Institute (CCTSI)
UNIVERSITY OF COLORADO DENVER | ANSCHUTZ MEDICAL CAM


Office of the Vice Chancellor for Research
UNIVERSITY OF COLORADO DENVER | ANSCHUTZ MEDICAL CAMPUS


Graduate School
UNIVERSITY OF COLORADO
ANSCHUTZ MEDICAL CAMPUS


Gates Institute
UNIVERSITY OF COLORADO
ANSCHUTZ MEDICAL CAMPUS


Genomics Core
University of Colorado - Anschutz Medical Campus


Innovations
UNIVERSITY OF COLORADO ANSCHUTZ MEDICAL CAMPUS


School of Medicine
UNIVERSITY OF COLORADO
ANSCHUTZ MEDICAL CAMPUS


Student Affairs
UNIVERSITY OF COLORADO
ANSCHUTZ MEDICAL CAMPUS


National Jewish Health
Breathing Science is Life.


Agilent


avantor
delivered by VWR


fisher scientific
part of Thermo Fisher Scientific


GeminiBio
Empowering cell culture and process liquid workflows®


METTLER TOLEDO


RAININ
Pipetting 360+


Thomas
Scientific


WATCHMAKER
GENOMICS